DESIGN AND FABRICATION OF PIEZOELECTRIC MICROVALVE FOR ULSI MICROFLUIDIC APPLICATION

IMRAN AHMAD

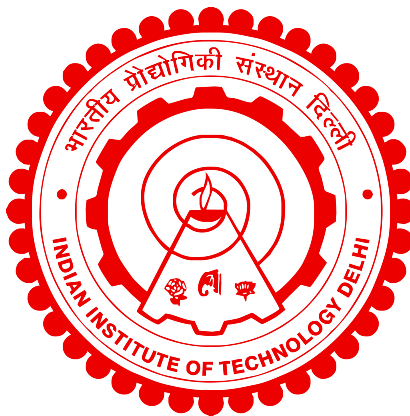

DEPARTMENT OF ELECTRICAL ENGINEERING

INDIAN INSTITUTE OF TECHNOLOGY DELHI

July 2025

© Indian Institute of Technology Delhi (IITD), New Delhi, 2025

DESIGN AND FABRICATION OF PIEZOELECTRIC MICROVALVE FOR ULSI MICROFLUIDIC APPLICATION

by

IMRAN AHMAD

Department of Electrical Engineering

Submitted

in partial fulfillment of the requirements of the degree of Doctor of Philosophy

to the

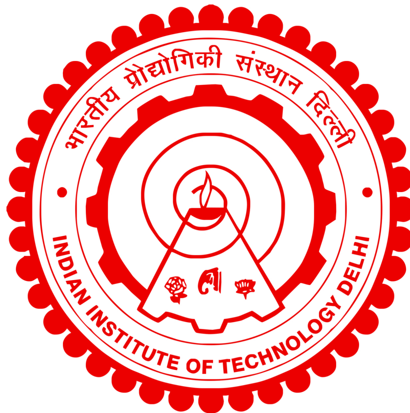

INDIAN INSTITUTE OF TECHNOLOGY DELHI

July 2025

Dedicated to my Parents

Certificate

This is to certify that the thesis entitled **"DESIGN AND FABRICATION OF PIEZOELECTRIC MICROVALVE FOR ULSI MICROFLUIDIC APPLICATION"**, submitted by **Mr. Imran Ahmad** to the Indian Institute of Technology Delhi, for the award of the degree of **Doctor of Philosophy**, is a record of the original, bonafide research work carried out by him under my supervision and guidance. The thesis has reached the standards fulfilling the requirements of the regulations related to the award of the degree.

The results contained in this thesis have not been submitted in part or in full to any other University or Institute for the award of any degree or diploma to the best of my knowledge.

Prof. Bhaskar Mitra
Associate Professor,
Department of Electrical Engineering,
Indian Institute of Technology Delhi,
New Delhi-110016, India.

Acknowledgements

I would like to thank my supervisor, Prof. Bhaskar Mitra, for their valuable guidance, advice, and encouragement throughout this research work. His passion for research and constant pursuit of quality, enthusiasm for technology, and vision for research direction have motivated me right from the beginning of my PhD. His profound expertise in fabrication of MEMS devices through state-of-the-art microfabrication techniques helped me a lot to achieve the objective of this thesis. His insightful guidance and unwavering support helped me throughout the research and writing of this thesis. I am grateful to my supervisor for proving an opportunity to work on a exciting intradisciplinary project.

I would also like to thank my research committee members, Prof. Madhusudan Singh, Prof. Dhiman Mallick, and Prof. Sitikantha Roy. Their informative remarks and valuable suggestions during the review of the research progress were crucial in enhancing this dissertation work. I also want to express my gratitude to Prof. Gufran Sayeed Khan (SeNSE), Prof. Ankur Goswami (MSE), Prof. Sandeep Jha (CBME), Prof. Neeraj Khare (Physics), Prof. Sujeet Kumar Sinha (Mech), and Prof. Divesh Bhatia (Chemical) for allowing me to access their lab facility.

I am grateful to be part of my multidisciplinary research group at IIT Delhi and want to thank my friends and colleagues especially Dr. Vikram Maharishi, Mr. Aamir Saud Khan, Dr. Satish Verma, Ms. Rumaysa Manzoor, Dr. Nitika Batra, Dr. Vasudha Agrwal, Dr. Priya Vinayak, Mr. Manjeet Kumar, Ms. Maninder Kaur, and Dr. Pawan Kumar for their companionship, support, and encouragement. I would also like to thank all members of the FMDL research group, especially Mr. Parvez Akhtar, Mr. Samim Reza, and Mr. Tejveer Singh Anand, and a special note of thanks to Dr. Henam Sylvia Devi for all the help and support in overseeing the execution of my experiments.

I appreciate the assistance provided by Ms. Shalini Singh, Mr. Vinit Yadav, Mr. Pankaj Pathak, Dr. Nadeem Tariq Beigh, Mr. Faizan Tariq Beigh, Mr. Taslim Khan and Mr. Umesh Gautam during different phases of my PhD. A heartfelt thanks to Mr. Ahmed Shaban and Dr. Sneha Kumari for their their companionship,unwavering support and encouragement, making this journey enjoyable and memorable.

I am profoundly thankful to my friends Mr. Arun Kumar Choudhary(Scientist-C, MNRE), Dr. Shubham Sahay (Assistant Professor, IIT Kanpur), Ms. Fran Tavares

(Entrepreneur), Dr.Gaurav Musalgaonkar (Micron) and Mr. Aamir Khan for their strong moral support and encouragement during my PhD journey.

I thank the Ministry of Education, Government of India, and the Department of Electrical Engineering, IIT Delhi, for their generous support through the PhD scholarship and access to advanced laboratory resources. I sincerely thank the Nano Research Facility (NRF) and the Central Research Facility (CRF) for providing cutting-edge device fabrication and characterization facilities. I want to acknowledge the support from all NRF-IIT Delhi staff members during this work. I also extend my gratitude to the staff in the Electrical Engineering office, particularly Mr. Rakesh Kumar, Mr. Yatindra and Mr. Satish, for all the official paperwork. I sincerely want to thank everyone with whom I had the privilege of working and who helped me directly or indirectly throughout this research work.

Finally and most importantly, I want to express my deepest gratitude to my mother, Mrs. Khatmoon Nisha, and my late father, Mr. Sharif Ansari, for their immense sacrifices, unwavering support, and selfless love. They have always encouraged me to strive for higher education and taught me the values of being a kind and compassionate human being. I especially want to thank my mother for being a pillar of strength and providing constant support throughout the ups and downs of my PhD journey. I would also like to thank my elder brothers, Mr. Perwej Ahamad and Dr. Khurshed Ahamad, for their love, affection, and continuous guidance from my school days. I want to express my profound appreciation to my wife, Mrs. Shahnaz, for her unwavering patience and support, which have sustained me throughout this challenging journey. A Special appreciation goes to my sisters-in-law Mrs. Rabia Ansari and Mrs. Tazeen Fatma, for their care and consistent encouragement throughout this journey. I would also like to thank my nieces, Arisha, Anabia, Harim,Nephew Mohammad Azlan and my son Izhaan Ahmad for bringing so much love, affection and joy into my life.

Imran Ahmad

Imran Ahmad

Abstract

Microfluidics technology has a lot of promise in Lab on chip, drug discovery and combinatorial chemistry applications. However, progess in many applications is hampered by the lack of a scalable, low cost and reliable valve technology. Pneumatically actuated valves have been the mainstay of microfluidic valve technology, but are hard to scale and require a supply of compressed air.

This dissertation focuses on the design, fabrication, and testing of a piezoelectric microvalve integrated with microfluidics through a transfer process. Firstly, a comprehensive study on lead-free materials like P(VDF-TrFE), potassium sodium niobate (KNN), and barium titanate ($BaTiO_3$) is undertaken. Various methods to create thin films, such as drop casting, spin coating, and screen printing, are explored. A low-temperature process to fabricate the valve using screen printing has been developed using a nanocomposite paste using $BaTiO_3$ nanopowder and ethyl cellulose. The screen-printed film has been characterized, showing good crystallinity, excellent piezoelectricity ($d_{33} \sim 370$ pm/V), and Young's modulus (2.54 GPa). The rheological analysis of the paste exhibits a pseudoplastic effect, which is essential for achieving high-quality printing with minimal force and preventing screen blockages.The electron probe microanalyzer (EPMA) was performed for quantitative analysis of elements present in nanocomposites paste, confirming homogeneous mixing and uniform spatial distribution of elements required to exhibit enhanced piezoelectricity.

Another lead-free piezoelectric nanocomposite materials consisting of P(VDF-TrFE) and KNN have been synthesized. The thin film of the nanocomposite has been characterized, showing good crystallinity and enhanced piezoelectric response ($d_{33} \sim$ 96 pm/V for composite-1 and $d_{33} \sim$ 95 pm/V for composite-2), an almost 2.5-fold increase compared to the d_{33} of pristine P(VDF-TrFE) film. Nanoindentation was performed to measure Young's modulus and the material's stiffness. The measured Young's modulus was 2.17 GPa for composite-1 and 2.97 GPa for composite-2. The measured stiffness^2/load was $\sim$ 71.9 GPa for composite-1 and 165 GPa for composite-2.

This thesis has demonstrated two methods for transferring a thin parylene membrane on top of the PDMS microfluidic channel by utilizing parylene-parylene bonding.

Furthermore, a novel low-temperature process for the fabrication of microvalves through screen printing has been developed and demonstrated successfully.

Finally, a straightforward low-temperature drop-casting method was utilized to fabricate piezoelectric microvalves using composite-1. The piezoelectric stack actuator was fabricated on a 2-inch silicon wafer using surface micromachining. The piezoelectric actuator was transferred to the PDMS microchannel through a transfer process for microvalve fabrication. The displacement of the parylene membrane in response to a DC voltage was characterized indirectly using a DC probe station and directly using a 3D optical profiler. The profiler characterization shows a maximum membrane deflection of $\sim 2.847\,\mu m$ at an actuation voltage of 12 V. Plane actuation was performed by introducing dye at the inlet and studying its flow behavior through optical microscopy to outlet at 12 V, 0 V, and –12 V, demonstrating valving action. The leakage pressure of the microvalve lies in the range of 32–34 kPa, suggesting that valve operation must be performed below this pressure for safe and reliable operation. The microvalve testing results are encouraging and hold significant promise for advancing microfluidic technologies and laboratory automation.

In summary, this dissertation work provides a novel approach to the fabrication of a piezoelectric microvalve and its integration with microfluidics using the transfer in a facile manner.

सार

माइक्रोफ्लुइडिक्स तकनीक में चिप प्रयोगशाला, दवा खोज और कॉम्बिनेटरियल रसायन विज्ञान अनुप्रयोगों में अपार संभावनाएं हैं। हालाँकि, कई अनुप्रयोगों में प्रगति एक मापनीय, कम लागत वाली और विश्वसनीय वाल्व तकनीक के अभाव के कारण बाधित है। वायवीय रूप से संचालित वाल्व माइक्रोफ्लुइडिक वाल्व तकनीक का मुख्य आधार रहे हैं, लेकिन इन्हें मापना कठिन है और इसके लिए संपीड़ित हवा की आपूर्ति की आवश्यकता होती है। यह शोध प्रबंध एक स्थानांतरण प्रक्रिया के माध्यम से माइक्रोफ्लुइडिक्स के साथ एकीकृत एक पीजोइलेक्ट्रिक माइक्रोवाल्व के डिज़ाइन, निर्माण और परीक्षण पर केंद्रित है। सबसे पहले, P(VDF–TrFE), पोटेशियम सोडियम नाइओबेट (KNN), और बेरियम टाइटेनेट ($BaTiO_3$) जैसे सीसा रहित पदार्थों पर एक व्यापक अध्ययन किया गया है। पतली फिल्में बनाने के विभिन्न तरीकों, जैसे ड्रॉप कास्टिंग, स्पिन कोटिंग और स्क्रीन प्रिंटिंग, का पता लगाया गया है। स्क्रीन प्रिंटिंग का उपयोग करके वाल्व बनाने की एक निम्न–तापमान प्रक्रिया विकसित की गई है। BaTiO3 नैनोपाउडर और एथिल सेलुलोज़ का उपयोग करके एक नैनोकंपोजिट पेस्ट का उपयोग किया गया है। स्क्रीन–प्रिंटेड फिल्म की विशेषताओं का विश्लेषण किया गया है, जिसमें अच्छी क्रिस्टलीयता, उत्कृष्ट पीजोइलेक्ट्रिसिटी (d33$\sim$370 pm/V) और यंग मापांक (2.54 GPa) प्रदर्शित हुए हैं। पेस्ट का रियोलॉजिकल विश्लेषण एक छद्मप्लास्टिक प्रभाव प्रदर्शित करता है, जो न्यूनतम बल के साथ उच्च–गुणवत्ता वाली प्रिंटिंग प्राप्त करने और स्क्रीन अवरोधों को रोकने के लिए आवश्यक है। इलेक्ट्रॉन प्रोब माइक्रोएनलाइज़र (EPMA) का उपयोग नैनोकंपोजिट पेस्ट में मौजूद तत्वों के मात्रात्मक विश्लेषण के लिए किया गया, जिससे बढ़ी हुई पीजोइलेक्ट्रिसिटी प्रदर्शित करने के लिए आवश्यक तत्वों के सजातीय मिश्रण और समान स्थानिक वितरण की पुष्टि हुई। P(VDF–TrFE) और KNN से युक्त एक और सीसा–रहित पीजोइलेक्ट्रिक नैनोकंपोजिट सामग्री का संश्लेषण किया गया है। नैनोकंपोजिट की पतली फिल्म की विशेषताएँ निर्धारित की गई हैं, जो अच्छी क्रिस्टलीयता और बढ़ी हुई दाबविद्युत प्रतिक्रिया (कम्पोजिट–1 के लिए d33 $\sim$96 pm/V और कम्पोजिट–2 के लिए d33 $\sim$95 pm/V) दर्शाती है, जो कि प्राचीन P(VDF–TrFE) फिल्म के d33 की तुलना में लगभग 2.5 गुना वृद्धि है। यंग मापांक और पदार्थ की कठोरता को मापने के लिए नैनोइंडेंटेशन किया गया। मापा गया यंग मापांक कम्पोजिट–1 के लिए 2.17GPa और कम्पोजिट–2 के लिए 2.97GPa था। मापी गई कठोरता2/भार कम्पोजिट–1 के लिए $\sim$71.9GPa और कम्पोजिट–2 के लिए 165GPa थी। इस शोध प्रबंध में पैरीलीन–पैरीलीन बंधन का उपयोग करके PDMS माइक्रोफ्लुइडिक चैनल के शीर्ष पर एक पतली पैरीलीन झिल्ली को स्थानांतरित करने की दो विधियों का प्रदर्शन किया गया है। इसके अलावा, स्क्रीन प्रिंटिंग के माध्यम से माइक्रोवाल्वों के निर्माण के लिए एक नवीन निम्न–तापमान प्रक्रिया विकसित और सफलतापूर्वक प्रदर्शित की गई है। अंततः, कंपोजिट–1 का उपयोग करके पीजोइलेक्ट्रिक माइक्रोवाल्वों के निर्माण हेतु एक सरल निम्न–तापमान ड्रॉप–कास्टिंग विधि का उपयोग किया गया। पीजोइलेक्ट्रिक स्टैक एक्ट्यूएटर का निर्माण सतह माइक्रोमशीनिंग का उपयोग करके 2–इंच सिलिकॉन वेफर पर किया गया था। माइक्रोवाल्व निर्माण हेतु एक स्थानांतरण प्रक्रिया के माध्यम से पीजोइलेक्ट्रिक एक्ट्यूएटर को PDMS माइक्रोचैनल में स्थानांतरित किया गया था। डीसी वोल्टेज की प्रतिक्रिया में पैरीलीन झिल्ली के

विस्थापन को अप्रत्यक्ष रूप से डीसी प्रोब स्टेशन का उपयोग करके और प्रत्यक्ष रूप से 3D ऑप्टिकल प्रोफाइलर का उपयोग करके चिह्नित किया गया था। प्रोफाइलर अभिलक्षणन 12 V के एक्चुएशन वोल्टेज पर लगभग 2.847 µm का अधिकतम झिल्ली विक्षेपण दर्शाता है। समतल एक्चुएशन इनलेट में डाई डालकर और 12 V, 0 V, और −12 V पर आउटलेट तक ऑप्टिकल माइक्रोस्कोपी के माध्यम से इसके प्रवाह व्यवहार का अध्ययन करके किया गया, जिससे वाल्विंग क्रिया का प्रदर्शन हुआ। माइक्रोवाल्व का रिसाव दबाव 32−34 kPa की सीमा में है, जो यह सुझाव देता है कि सुरक्षित और विश्वसनीय संचालन के लिए वाल्व संचालन इस दबाव से नीचे किया जाना चाहिए। माइक्रोवाल्व परीक्षण के परिणाम उत्साहजनक हैं और माइक्रोफ्लुइडिक प्रौद्योगिकियों और प्रयोगशाला स्वचालन को आगे बढ़ाने के लिए महत्वपूर्ण संभावनाएं रखते हैं।संक्षेप में, यह शोध प्रबंध एक पीजोइलेक्ट्रिक माइक्रोवाल्व के निर्माण और स्थानांतरण का उपयोग करके माइक्रोफ्लुइडिक्स के साथ इसके एकीकरण के लिए एक नया दृष्टिकोण प्रदान करता है।

Contents

Certificate **i**

Acknowledgements **ii**

Abstract **iv**

Contents **viii**

List of Figures **xii**

List of Tables **xvi**

Abbreviations **xvii**

1 Introduction **1**

1.1 Overview 1
1.2 Literature review 3
1.3 Classification of Microvalves 4
1.3.1 Normally open and Normally closed Microvalves 5
1.3.2 Active and Passive Microvalves 5
1.3.3 Actuation Methods 7
1.3.3.1 Electromagnetic Actuation 7
1.3.3.2 Electrostatic Actuation 7
1.3.3.3 Piezoelectric Actuation 8
1.3.3.4 Thermal Actuation 8
1.3.3.5 Shape Memory Alloy Actuation 9
1.3.3.6 PDMS-Based Pneumatic Microvalve or Quake valve 10
1.4 Piezoelectricity 10
1.4.1 Objectives 13
1.5 Thesis Organisation 14

2 Exploring Lead-Free Piezoelectric Materials for Microvalve Fabrication 17
2.1 Introduction 17
2.2 Potassium Sodium Niobate (KNN) film 19
2.2.1 Synthesis of KNN 19
2.2.2 Deposition using Spin-Coating 21
2.2.3 Characterization of Piezoelectric Response in KNN 22
2.3 Synthesis and Deposition of P(VDF-TrFE) Thin Film 22
2.3.1 Characterization of P(VDF-TrFE) Film 23
2.3.2 Piezo Response of 10 wt % P(VDF-TrFE) 24
2.4 **Synthesis and Characterization of Lead-Free $BaTiO_3$ Paste for Screen-Printing** 25
2.4.1 Background and Motivation 25
2.4.2 Materials and Methods 26
2.4.2.1 Synthesis of Paste for Screen Printing using **$BaTiO_3$** Nano Powder 26
2.4.2.2 Barium Titanate Film Characterization 27
2.4.3 Results and Discussion 29
2.4.3.1 Rheological Analysis of Paste to Study Flow Behaviour 29
2.4.3.2 Material Characterization of Barium Titanate Film prepared by Screen Printing 30
2.4.3.3 Piezo Response Force Microscopy (PFM) 32
2.4.3.4 Electron Probe Micro Analysis of the Composite Film 33
2.5 Summary 35

3 Study of Weight Ratio-based Optimization of P(VDF-TrFE): KNN Composites for Enhanced Piezoelectric Response 36
3.1 Introduction 36
3.2 Experimental Methods 39
3.2.1 Synthesis of P(VDF-TrFE) and KNN Composite 39
3.2.2 Nano Composite Thin Film Characterization 41
3.3 Results and Discussion 42
3.3.1 Material Characterization of Composite 42
3.3.2 Surface Analysis of Thin Film prepared by Drop Cast 45
3.3.3 Piezo Response Force Microscopy (PFM) 47
3.3.4 Polarization vs. Electric Field Analysis 48
3.4 Summary 49

4 Fabrication of Piezoelectric Microvalve using Screen Printing Through Transfer Process 50
4.1 Introduction 50

4.2 Experimental Process Steps for Microvalve Fabrication 52
4.3 Fabrication for Microfluidic Channel 53
4.3.1 Rectangular Cross-Section Channel 53
4.3.2 Round Cross-Section Channel 54
4.3.3 Fabrication of Elastomeric stamp of PDMS through Soft Lithography 56
4.4 Membrane Transfer 57
4.4.1 Membrane Transfer Process using Silicon 59
4.4.2 Membrane Transfer using a Teflon Carrier 59
4.5 Design and Simulation 60
4.5.1 Device Design 60
4.5.2 Simulation Result 61
4.6 Screen Printing of Piezoelectric Actuator 62
4.7 Results and Discussion 64
4.7.1 Fabrication Results 64
4.7.2 Experimental results and measurement with DC probe station to characterize the membrane deflection 64
4.7.3 Valve displacement measurement using 3D Optical Profilometer 66
4.8 Summary 69

5 Fabrication of Microvalve Integrated Microfluidics by Drop Cast Through Transfer Process 70
5.1 Introduction 70
5.2 Experimental Process Steps for Microvalve Fabrication 71
5.3 Design and Simulation 72
5.3.1 Device Design 73
5.3.2 Simulation result 74
5.4 Results and Discussion 75
5.4.1 Plasma Surface Treatment on Hydrophobic Substrate of Parylene C to achieve Thin Film of Composite 75
5.4.2 Fabrication Results of the Piezoelectric Microvalve by Drop Cast 76
5.4.3 Experimental Results and Measurement with DC Probe Station to Characterize the Membrane Deflection 78
5.4.4 Valve Displacement Measurement using 3D Optical Profilometer 79
5.4.5 Optical Characterization of Plane Valve Actuation 82
5.4.6 Experimental Setup and Results for Back and Leakage Pressure of Microvalve 82
5.4.7 Microfluidic Valve Test Results 84
5.4.8 Leakage Pressure Measurement with different syringe sizes . . 86
5.5 Summary 87

6 Conclusion and Future Scope **89**
6.1 Conclusion . . . 89
6.2 Future Scope . . . 90

Conclusion and Future Scope **91**

A Fabrication of a Piezoelectric Actuator for Microvalve Fabrication using the Transfer Process **91**
A.1 Overview . . . 91
A.2 Introduction . . . 92
A.3 Materials and Methods . . . 93
A.4 Fabrication Process of the Valve using a Transfer Process . . . 95
A.5 Result and Discussion . . . 96
A.5.1 Fabrication of Microfluidic Channel . . . 96
A.5.2 Parylene Membrane Transfer . . . 97
A.5.2.1 Fabrication Result . . . 98
A.6 Conclusion . . . 99

B Measured Step Height of Membrane with Optical Profiler **100**

C A Novel Method for Reversible Bonding by Surface Charges Implanted on Parylene Film Through Corona Discharge **106**
C.1 Overview . . . 106
C.2 Introduction . . . 107
C.3 Process Flow of Surface charge Trap on Parylene C Thin Film . . . 109
C.3.1 Fabrication of microfludics channel . . . 109
C.3.2 Membrane Transfer using Trasfer Tape . . . 110
C.4 Experimental Setup . . . 110
C.5 Result and Discussion . . . 112
C.6 Conclusion . . . 112

Bibliography **115**

List of Publications **135**

Curriculum Vitae **137**

List of Figures

1.1 Schematic illustrating a piezoelectric microvalve consisting of a PDMS microchannel, parylene membrane, and stacked piezoelectric disk actuator. . . . 3

1.2 Pneumatic microvalve: (a) Normally open valve [1] (b) Normally closed valve [43] (c) Lifting gate normally closed [44]. . . . 6

1.3 Passive valves: (a) cantilever and (b) bridge-type passive check valves. [45] . . . 6

1.4 Actuation mechanisms in microvalves: (a) Electromagnetic (b) Electrostatic (c) Piezoelectric (d) Bimetallic (e) Thermonumatic (f) SMA actuation (g) Illustrating typical pressure and response times of different actuators utilized in microvalves. . . . 9

1.5 (a) Optical Image of Quake On/Off Valve (b) Schematic of Quake Micropump (c) Closing of Trapezoidal Channel at 200 kPa (d) Closing a round cross section with the exact dimensions as a trapezoidal channel can be achieved with a significantly lower pressure of 40 kPa. [1] . . . 11

1.6 (a) The Direct Piezoelectric Effect (b) The Inverse Piezoelectric Effect (d) Effect of poling in an unpoled material. [54] . . . 12

2.1 Schematic of the Process Steps for the Synthesis of KNN . . . 20

2.2 (a) and (b) Optical and 3D optical profiler image of film at 2000 RPM; (c) and (d) Optical and 3D optical profile image of film at 3000 RPM. . . . 21

2.3 Illustration of Piezo response Force Microscopy (PFM) characteristics of the KNN film: (a) amplitude as a function of tip bias and (b) phase variation with tip bias. . . . 22

2.4 Material Characterization: (a) SEM image (b) AFM image (c) FTIR (d) XRD of film show crystalline β phase. . . . 24

2.5 Illustration of Piezo response Force Microscopy (PFM) characteristics of the P(VDF-TrFE) film: (a) Amplitude as a function of tip bias and (b) Phase variation with tip bias. . . . 25

2.6 Schematic of the synthesis process of paste for screen printing . . . 26

2.7 Rheology of barium titanate paste: (a) Viscosity profile of paste (b) Flow curve of paste. . . . 29

2.8 Material Characterization: (a) XRD shows good crystallinity; (b) Raman spectra; (c) and (d) TEM images at different scales for particle size analysis. 31
2.9 PFM analysis: (a) amplitude vs tip bias and (d) phase vs tip bias. . . 33
2.10 EPMA analysis shows the uniform elemental distribution of $BaTiO_3$ particles throughout the ethyl cellulose matrix (a) Optical Image Scanning area of printed Pizo disc (b) Oxygen-O_2 (b) Carbon-C (d) Titanium-Ti (e) Barium (f) Elemental Overlay. 34

3.1 (a) Schematic of the synthesis process (b) Two different composites were prepared by varying P(VDF-TrFE) weight percentage (c) Drop cast for a piezoelectric film of the composite after plasma treatment. . 40
3.2 Material Characterization of all wt % P(VDF-TrFE)-KNN composites: (a) XRD (b) FTIR (c) Raman Spectra, (d) Nanoindentation, (e) EDX elemental mapping of composite-1 (f) EDX elemental mapping of composite-2. 45
3.3 Morphological Analysis of the film using AFM and SEM (a) 5 wt% P(VDF-TrFE) (b) Composite-1 (c) 10 wt% P(VDF-TrFE) (d) Composite-2. 46
3.4 (a) and (b) Amplitude and Phase response of Composite-1 (c) and (d) Amplitude and Phase response of Composite-2. 48
3.5 PE Loop of (a) 5wt% (b) 10 wt% P(VDF-TrFE)- KNN (30 vol%). . . 48

4.1 Process flow of valve fabrication by screen printing: (a) Disk piezoelectric-stack fabrication (b) transfer of piezo stack on top of a PDMS microchannel. 53
4.2 Microfluidic channel fabrication (a) Image of the fabricated mask on chrome plate (b) Process flow for SU8 pattering (c) Optical Image of the rectangular microfluidic channel. 54
4.3 Microfluidic channel fabrication: (a) Optical image of the channel before resist reflow; (b) Optical image of the channel after resist reflow; (c) SEM image of fabricated round microfluidic channel. 55
4.4 Image of fabricated stamp of PDMS after soft lithography. 57
4.5 (a) Process flow for membrane transfer using Si-wafer; (b) Parylene-Parylene bonding at 230°C; (c) Transferred Parylene membrane using Si-wafer. 58
4.6 Process flow of membrane transfer using Teflon (c)Transferred parylene membrane using Teflon. 60
4.7 (a) COMSOL FEM Model (b) Effect of piezoelectric layer thickness (c) Effect of parylene membrane thickness (d) Effect of piezoelectric layer diameter on membrane displacement. 62
4.8 (a) Screen of mesh size 170; (b) Screen and wafer alignment; (c) Printed piezoelectric disc. 63

4.9 Fabrication results (a) Image demonstrating fabrication of piezo-stack (b) Image demonstrating the transfer process of the stack to the microchannel (c) Optical Image of the printed disc of barium titanate (d) Top view optical image of the fabricated microvalve 65
4.10 Fabrication results (a) Image demonstrating fabrication of piezo-stack (b) Image demonstrating the transfer process of the stack to the microchannel (c) Optical Image of the printed disc of barium titanate (d) Top view optical image of the fabricated microvalve. 66
4.11 Experimental set-up for valve membrane deflection with DC voltage supply. 67
4.12 3D-optical profilometer and wire-bonded microvalve. Measurement of relative displacement of membrane between step height at (a) 0V and (b) 15V. 68

5.1 Process flow of (a) fabrication of the piezoelectric actuator and (b) transfer process of the actuator to the microfluidics channel. 73
5.2 (a) COMSOL FEM Model (b) Effect of piezoelectric layer thickness (c) Effect of parylene membrane thickness (d) Effect of piezoelectric layer diameter on membrane displacement. 75
5.3 Contact angle measurement (a) 58.1° after drop cast (b) reduces to 21.3° after plasma treatment. 76
5.4 Optical image: (a) bottom electrode, (b) drop cast composite, (c) PVD of Au for top contact, and (d) image of the fabricated actuator using drop cast technique. 77
5.5 Transfer Process: (a) Thermal release of stack, (b) Alignment and bonding to channel, and (c) Released microvalve after transfer of piezoelectric stack. 77
5.6 (a) DC Probe station to measure the air gap capacitance to characterize membrane deflection (b) Measured capacitance in response to applied DC voltage. 79
5.7 Experimental setup for valve membrane deflection with DC voltage supply, 3D optical profilometer, and wire-bonded microvalve. 79
5.8 (a) Measured step height 42.471 µm at 0 V (b) Measured step height decreases to 39.624 µm at 12 V in response to membrane downward displacement. 80
5.9 Parylene membrane relative displacement with applied voltage. . . . 81
5.10 (a) Experimental setup to test plane actuation of the microvalve (b) Priming of the valve with DI water was performed to remove air bubbles trapped inside the channel before operation (c) After priming, the valve is actuated at 12 V, and red dye is added to the inlet. (d) The actuation voltage is set to 0V, which means that the valve is open (e) The valve is de-actuated by applying -12 V. 83
5.11 Experimental Setup for Back and Leakage Pressure Measurement. . . 84

5.12 (a) Output voltage of pressure sensor recorded in an oscilloscope; (b) Plot of back pressure concerning increase in flow rate of fluid flowing inside the microchannel. 85
5.13 Output voltage of the pressure sensor recorded in an oscilloscope with an increase in syringe size. 86
5.14 Plot of leakage pressure with respect to increase in syringe size. . . . 87

A.1 Schematic of piezoelectric valve assembly. 93
A.2 (a) SEM image of the film; (b) AFM topography image of the film; (c) FTIR spectrum; (d) XRD of the film. 94
A.3 (a) Process flow of disk piezoelectric-stack fabrication (b) Transfer process of the stack to the PDMS. 96
A.4 Optical image of the fabricated microfluidic channel by using negative photoresist SU8 2035. 97
A.5 Optical image of PDMS microchannels with transferred parylene membrane. 98
A.6 Optical image of fabricated piezoelectric actuator. 99

B.1 Measured step height 42.471 µm at 0V. 101
B.2 Measured step height 41.907 µm at 2V. 101
B.3 Measured step height 41.443 µm at 4V. 102
B.4 Measured step height 40.955 µm at 6V. 102
B.5 Measured step height 40.548 µm at 8V. 103
B.6 Measured step height 40.323 µm at 10V. 103
B.7 Measured step height 39.624 µm at 12V. 104
B.8 Measured step height 39.728 µm at 14V. 104
B.9 Measured step height 40.376 µm at 16V. 105

C.1 Schematic of the Corona discharge method for surface charge implantation. 108
C.2 Process Flow (a) Parylene membrane transfer (b) Postive and negative charge implanted on parylene film. 109
C.3 Optical image of fabricated channel with negatibe PR-SU8-2035. . . . 110
C.4 Optical image of transferred parylene film using TPE bonding. 111
C.5 Experimental setup of surface charging using corona discharge. 112
C.6 (a) Set-up of SPV measurement of PDMS chip with transferred parylene membrane; (b) Measured surface potential in volts; (c) Sample reversibly bonded by electrostatic force between positively and negatively implanted charges on parylene surface by the Corona discharge method. 113

List of Tables

2.1 Piezoelectric properties of different materials. 19

3.1 Material composition of prepared composites 40
3.2 Surface roughness of pristine P(VDF-TrFE) film and composite films 46

4.1 Material properties used for FEM Analysis 61

5.1 Material properties used for FEM Analysis 74
5.2 Measured displacement with increasing DC voltage 84
5.3 Measured output voltage of pressure sensor and corresponding back pressure 85
5.4 Output voltage of pressure sensor and corresponding leakage pressure 87

Abbreviations

MEMS	Micro-Electro-Mechanical Systems
PZT	Lead Zirconate Titanate
$BaTiO_3$	Barium Titanate
KNN	Potassium Sodium Niobate
PVDF-TrFE	Poly(vinylidene fluoride–trifluoro ethylene)
PDMS	Polydimethylsiloxane
Parylene	Poly-para-xylylene
PR	Photoresist
PFM	Piezoresponse Force Microscopy
DI	Deionized Water
IPA	Isopropyl Alcohol
UV	Ultraviolet
TEM	Tunnelling Electron Microscope
SEM	Scanning Electron Microscope
FESEM	Field Emission Scanning Electron Microscope
EPMA	Electron Probe Microanalyser
XRD	X-ray Diffraction
EDX	Energy Dispersive X-ray Spectroscopy
FTIR	Fourier Transform Infrared Spectroscopy
Raman	Raman Spectroscopy
AFM	Atomic Force Microscope
RIE	Reactive Ion Etching
LDV	Laser Doppler Vibrometer
DC	Direct Current
CVD	Chemical Vapour Deposition
CV	Capacitance–Voltage

IV	Current–Voltage
Si	Silicon
NO	Normally Open
NC	Normally Closed
Mo	Molybdenum
Al	Aluminium
Au	Gold
d_{33}	Piezoelectric Charge Coefficient
ε_{33}	Dielectric Constant
FEA	Finite Element Analysis
SU8 2030	Negative Photoresist
AZ 40XT	Positive Photoresist
P-E	Polarization–Electric Field
SMA	Shape Memory Alloy
PTFE	Polytetrafluoroethylene
Teflon-AF	Amorphous Fluoropolymer
DMSO	Dimethyl Sulfoxide